Available online at www.sciencedirect.com
SCIENCE DIRECT®
Journal of Sound and Vibration 274 (2004) 91–109
JOURNAL OF SOUND AND VIBRATION
www.elsevier.com/locate/jsvi

On the dynamics of piezoelectric cylindrical shells

M. Berg, P. Hagedorn*, S. Gutschmidt

Department of Applied Mechanics, Darmstadt University of Technology, Hochschulstr. 1, 64289 Darmstadt, Germany

Received 19 May 2003; accepted 19 May 2003

Abstract

In the present paper new equations of motion are derived for the vibration of piezo-ceramic thin-walled cylindrical shells, generalizing Flügge's shell theory for this type of material. These new equations differ from the ones known from the literature in that here the electric field is not assumed as constant over the thickness but is obtained by solving an additional differential equation in the thickness direction. The shells are polarized in the radial direction and the electrodes are in the form of identical sectors. Such shells are used e.g. as stators in some piezoelectric ultrasonic travelling wave motors and it is therefore important to study their free and forced vibrations.

The momentum and moment of momentum balance used in Flügge's shell theory are of course unchanged. The constitutive relations used in the theory of elastic shells are replaced by those of a linear piezoelectric material, so that additional field variables are introduced. These are subject to Maxwell's laws, which in particular have to be fulfilled by the electric field inside the shell. For a thin radially polarized shell, only dielectric displacements in the radial direction are taken into account. Due to the absence of free electric charges in dielectric media such as PZT, the divergence of the dielectric displacement vanishes. This condition leads to an ordinary differential equation of the Euler type in the radial electric field, which can be solved in closed form. Together with the thin shell assumptions and with the piezoceramic constitutive equations, this results in the equations of motion for thin piezoceramic shells with non-constant electric field over the thickness.

1. Introduction

This study of piezoelectric shells was motivated by their use in piezoelectric travelling wave motors, as described in Refs. [1,2]. In these motors, the stator is driven by an externally applied electric voltage, applied to its electrodes, generating a travelling bending wave via the inverse

*Corresponding author. Tel.: +49-6151-16-2185; fax: +49-6151-16-4125.
E-mail address: hagedorn@mechanik.tu-darmstadt.de (P. Hagedorn).

0022-460X/$ - see front matter © 2003 Elsevier Ltd. All rights reserved.
doi:10.1016/S0022-460X(03)00650-3

piezoelectric effect. In the present paper, Flügge's theory for elastic shells is generalized to cylindrical piezoelectric shells, as used in the travelling wave motors described in Refs. [1,2].

The shells are polarized in the radial direction and the electrodes are in the form of identical sectors. Such shells are used e.g. as stators in some piezoelectric ultrasonic travelling wave motors and it is therefore important to study their free and forced vibrations.

There are of course many technical publications on the modelling of piezoelectric structures, in particular beams, plates and shells, e.g. Refs. [3–7]. Beams, plates and shells are often assumed as elastic and thin piezoelectric elements are then bonded to the elastic structures. All these publications assume an electric field $E = V/t$ constant over the thickness. Therefore, the influence of the strain on the electric displacement must be neglected to fulfill Maxwell's law div $\mathbf{D} = 0$. The resulting error is negligible if the thickness of the piezoelectric element is small compared to the thickness of the complete structure. If this is not the case, a more refined model is needed and the earlier results cannot always be transferred to monolythic structures of piezoceramic material.

Publications [4,5,7] deal with beams while Refs. [5–7] deal with plates. In shells, the assumption of a constant electric field cannot fulfill Maxwell's law, even if the influence of the strain on the electric displacement is negligible. There was thus a need to derive a model covering monolythic shell structures with non-constant electric field over the thickness. This is an alternative to using of 3-D FEM calculations for shells and gives a useful engineering tool for a number of problems involving piezoelectric actuators. It also offers a basis for the formulation of a new type of finite element with a non-constant electric field. Such elements might be used for 2-D FEM calculations of piezoelectric, monolythic structures and piezoelectric shells.

Section 2 describes Flügge's model for isotropic material which forms the basis of the mathematical model of the piezoceramic shell. It is followed by an extension incorporating the special features of piezoelectric materials.

The boundary value problem is solved for harmonic electrical excitation in Section 3. Section 4 deals with the calculation of the electrical admittance of the piezoceramic shell. Some numerical results, namely axial displacements at the first eigenfrequency and electrical admittances are presented in Section 5 and compared to experimental values. A brief summary and an outlook are provided at the end of the paper.

2. Flügge's shell equations and their generalization to piezoelectric material

In 1934, Flügge presented a model for the dynamics of circular cylindrical shells with finite bending stiffness [8,9] for isotropic material. In what follows, the derivation of Flügge's equations is recalled. Then in a second step, Flügge's equations are generalized for a piezoceramic material including the electromechanical coupling and additional field variables. Different approximations for the fulfillment of Maxwell's equations are considered and compared.

2.1. The piezoelectric cylindrical shell

The stator of the motor described in Ref. [1] is a monolithic, piezoceramic shell which is covered with a closed thin electrode on the inner surface and nine evenly divided electrodes on the outer surface. This is also the shell considered in this paper. The geometry of the piezoceramic shell is

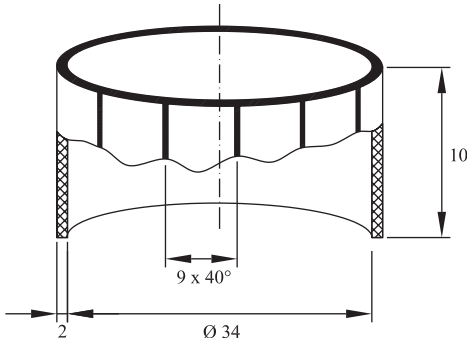

Fig. 1. Piezoceramic shell dimensions (in mm).

given by the height of 10 mm, the radius to the mid-surface of 18 mm, and the thickness of 2 mm (Fig. 1). The shell will be considered ideally rotationally symmetric with respect to mass distribution and stiffness, and the electrodes will only be considered in the application of the electric field. Each third metal strip is connected to form one electrode. So that this shell has three sets of electrodes for generating a travelling wave in the piezoelectric shell.

2.2. Flügge's shell theory

In the derivation of Flügge's equations, the following assumptions for cylindrical shells are made:

- All points that lie on a normal to a middle surface before deformation do the same after deformation.
- Displacements are small compared to the shell thickness.
- The normal stresses in the thickness direction are negligible (planar state of stress).

In particular, the first assumption may not correspond to reality in the neighborhood of the shell boundaries. However, this fact will not be considered here.

In the sequel, the indices x or 1 will denote the axial direction, while φ or 2 correspond to the circumferential and r or 3 to the radial direction. The cylindrical co-ordinates will be denoted correspondingly by x, φ and r and the displacements in these three directions by u, v and w respectively. The radius of the mid-surface of the circular cylinder is denoted by a, the thickness of the shell by s. The co-ordinate z denotes the distance of a point to the mid-surface so that $r = z + a$, or $z = r - a$.

In order to avoid confusion with the notation for derivatives, they are denoted by commas followed by indices, as is frequently done in the literature. In the case of functions of one variable only, we will however use the superscript "′". In addition, the non-dimensional axial co-ordinate $\vartheta = x/a$ is introduced, in order to simplify the equations. External loads acting on the shell are denoted by p_x, p_φ, p_r.

The stress resultants acting on an infinitely small shell element are shown in Fig. 2. The following six momentum and moment of momentum conditions can be formulated for

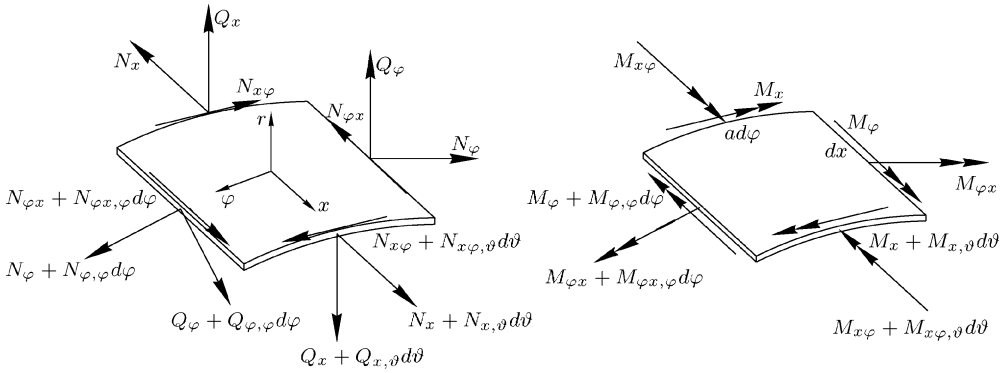

Fig. 2. Stress resultants on a shell element.

this element:

$$N_{x,\vartheta} + N_{\varphi x,\varphi} + ap_x = \mu a\ddot{u}, \tag{1}$$

$$N_{\varphi,\varphi} + N_{x\varphi,\vartheta} - Q_\varphi + ap_\varphi = \mu a\ddot{v}, \tag{2}$$

$$-Q_{\varphi,\varphi} - Q_{x,\vartheta} - N_\varphi + ap_r = \mu a\ddot{w}, \tag{3}$$

$$M_{\varphi,\varphi} + M_{x\varphi,\vartheta} - aQ_\varphi = 0, \tag{4}$$

$$M_{x,\vartheta} + M_{\varphi x,\varphi} - aQ_x = 0, \tag{5}$$

$$aN_{x\varphi} - aN_{\varphi x} + M_{\varphi x} = 0. \tag{6}$$

Here, the effects of rotatory inertia was neglected and the abbreviation $\mu = \rho s$ was used for the mass per unit area. The distributed forces and moments are related to the stresses via

$$N_\varphi = \int_{-s/2}^{s/2} \sigma_\varphi \, \mathrm{d}z, \tag{7}$$

$$N_x = \int_{-s/2}^{s/2} \sigma_x \left(1 + \frac{z}{a}\right) \mathrm{d}z, \tag{8}$$

$$N_{\varphi x} = \int_{-s/2}^{s/2} \tau_{x\varphi} \, \mathrm{d}z, \tag{9}$$

$$N_{x\varphi} = \int_{-s/2}^{s/2} \tau_{x\varphi} \left(1 + \frac{z}{a}\right) \mathrm{d}z, \tag{10}$$

$$M_\varphi = -\int_{-s/2}^{s/2} \sigma_\varphi \; z \, \mathrm{d}z, \tag{11}$$

$$M_x = -\int_{-s/2}^{s/2} \sigma_x \left(1 + \frac{z}{a}\right) z \, \mathrm{d}z, \tag{12}$$

$$M_{\varphi x} = -\int_{-s/2}^{s/2} \tau_{x\varphi} \, z \, \mathrm{d}z, \tag{13}$$

$$M_{x\varphi} = -\int_{-s/2}^{s/2} \tau_{x\varphi} \left(1 + \frac{z}{a}\right) z \, \mathrm{d}z \tag{14}$$

(see Ref. [8]). The stresses appearing on the right-hand side of Eqs. (7)–(14) are related to the strains through

$$\sigma_\varphi = \frac{E}{(1-\nu^2)} (\varepsilon_\varphi + \nu \varepsilon_x), \tag{15}$$

$$\sigma_x = \frac{E}{(1-\nu^2)} (\varepsilon_x + \nu \varepsilon_\varphi), \tag{16}$$

$$\tau_{x\varphi} = \frac{E}{2(1+\nu)} \gamma_{x\varphi} \tag{17}$$

in the case of elastic isotropic materials (planar state of stress). The strains on the other hand can be expressed through the displacements of the points on the mid-surface, using the kinematics according to Flügge's assumptions:

$$\varepsilon_x = \frac{u_{,\vartheta}}{a} - z \frac{w_{,\vartheta\vartheta}}{a^2}, \tag{18}$$

$$\varepsilon_\varphi = \frac{v_{,\varphi}}{a} - \frac{z}{a} \frac{w_{,\varphi\varphi}}{(a+z)} + \frac{w}{(a+z)}, \tag{19}$$

$$\gamma_{x\varphi} = \frac{u_{,\varphi}}{(a+z)} + \frac{(a+z)}{a^2} v_{,\vartheta} - \frac{w_{,\vartheta\varphi}}{a} \left(\frac{z}{a} + \frac{z}{(a+z)}\right). \tag{20}$$

Details can be found in Ref. [8]. The kinematical relations (18)–(20) together with the stress–strain relations (15)–(17) can now be used in Eqs. (7)–(14) to express the distributed forces and moments linearly through the mid-plane displacements and its derivatives. Next, these are substituted into Eqs. (1)–(6). Note that here the shear forces Q_x, Q_φ can be eliminated using Eqs. (4), (5) so that only Eqs. (1)–(3), and (6) remain.

However, Eq. (6) is automatically fulfilled due to the symmetry of the stress tensor. The integrations in Eqs. (7)–(14) lead to logarithmic terms like $\ln(2a - s) - \ln(2a + s)$. Since the whole shell theory is evaluated linearly, the logarithmic terms are replaced by the first two members of a Taylor series, so that $\ln(2a - s) - \ln(2a + s)$ becomes $(-s/a - s^3/12a^3)$. Substituting Eqs. (7)–(14) into the remaining equilibrium conditions finally leads to Flügge's differential equations for the

dynamics of circular cylindrical shells:

$$\frac{D}{a}\Bigg[u_{,\vartheta\vartheta}+\frac{(1-\nu)}{2}u_{,\varphi\varphi}+\frac{(1+\nu)}{2}v_{,\vartheta\varphi}+\nu w_{\vartheta} +\frac{s^2}{12a^2}\left(\frac{(1-\nu)}{2}u_{,\varphi\varphi}-w_{,\vartheta\vartheta\vartheta}+\frac{(1-\nu)}{2}w_{,\vartheta\varphi\varphi}\right)\Bigg]=\mu a\ddot{u}-ap_x, \tag{21}$$

$$\frac{D}{a}\Bigg[\frac{(1+\nu)}{2}u_{,\vartheta\varphi}+u_{,\varphi\varphi}+\frac{(1+\nu)}{2}v_{,\vartheta\vartheta}+w_{,\varphi} +\frac{s^2}{12a^2}\left(\frac{3}{2}(1-\nu)v_{,\vartheta\vartheta}-\frac{(3-\nu)}{2}w_{,\vartheta\vartheta\varphi}\right)\Bigg]=\mu a\ddot{v}-ap_{\varphi}, \tag{22}$$

$$\frac{D}{a}\Bigg[-\nu u_{,\vartheta}-v_{,\varphi}-w-\frac{s^2}{12a^2}\left(\frac{(1-\nu)}{2}u_{,\vartheta\varphi\varphi}-u_{,\vartheta\vartheta\vartheta}-\frac{(3-\nu)}{2}v_{,\vartheta\vartheta\varphi} +w_{,\vartheta\vartheta\vartheta\vartheta}+2w_{,\vartheta\vartheta\varphi\varphi}+w_{,\varphi\varphi\varphi\varphi}+2w_{,\varphi\varphi}+w\right)\Bigg]=\mu a\ddot{w}-ap_r, \tag{23}$$

where the abbreviation

$$D=\frac{Es}{(1-\nu^2)} \tag{24}$$

was used for the bending stiffness.

2.3. Piezoelectric shells

For piezoelectric shells the ''dynamic equilibrium conditions'' (1)–(6) remain unchanged. The same holds for the expressions of the stress resultants given in Eqs. (7)–(14). The change occurs in the constitutive relations, which in Eqs. (15)–(17) were given for an elastic material (non-piezoelectric) for the case of a planar state of stress.

The linear constitutive equations of a linear piezoelectric material in the general case of an arbitrary state of stress are given by Ikeda in [10] as

$$\mathbf{T}=\mathbf{c}^E\mathbf{S}-\mathbf{e}^{\mathrm{T}}\mathbf{E}, \tag{25}$$

$$\mathbf{D}=\mathbf{e}\mathbf{S}+\boldsymbol{\epsilon}^S\mathbf{E}, \tag{26}$$

where $\mathbf{T}$ is a (6×1) column matrix representing the mechanical stresses, $\mathbf{S}$ a (6×1) strain column matrix, $\mathbf{E}$ a (3×1) electric field vector and $\mathbf{D}$ a (3×1) vector of electric displacements. The elements of the matrices $\mathbf{c}^E$ (6×6), $\mathbf{e}^{\mathrm{T}}$ (6×3) and $\boldsymbol{\epsilon}^S$ (3×3) are material constants. The constitutive equations can be formulated with different sets of independent mechanical and electrical variables. The choice depends on the relative merits regarding the formulation of the boundary conditions [11].

In what follows, the electric boundary conditions will be formulated by locally prescribing the electric potential. This corresponds to electrically forced vibrations by applied voltages, or to free vibrations in the case of short-circuited electrodes. The resonance peaks in the electrical admittance functions then correspond to the eigenfrequencies of the shell with short-circuited

electrodes. Open electrodes, on the other hand, lead to (integral) boundary conditions formulated in terms of the electrical charges. The corresponding eigenfrequencies are associated with the antiresonances in the admittances.

Using the same assumptions as in Section 2.2, the relations between the planar stresses and strains

$$\sigma_\varphi = \frac{(c_{12}c_{33} - c_{13}^2)}{c_{33}}\varepsilon_x + \frac{(c_{11}c_{33} - c_{13}^2)}{c_{33}}\varepsilon_\varphi + \frac{d_{13}}{c_{33}}(2c_{13}^2 - (c_{11} + c_{12})c_{33})E_3, \tag{27}$$

$$\sigma_\varphi = \frac{(c_{11}c_{33} - c_{13}^2)}{c_{33}}\varepsilon_x + \frac{(c_{12}c_{33} - c_{13}^2)}{c_{33}}\varepsilon_\varphi + \frac{d_{13}}{c_{33}}(2c_{13}^2 - (c_{11} + c_{12})c_{33})E_3 \tag{28}$$

and

$$\tau_{x\varphi} = \frac{(c_{11} - c_{12})}{2}\gamma_{x\varphi} \tag{29}$$

are obtained from Eq. (25) for a piezoelectric material of type PIC141 (see the appendix). It is clear that the elastic anisotropy is not relevant here, since the piezoceramic shell is radially polarized. The material constants c_{kl}, d_{ij} coincide with the parameters given by the manufacturers in Cartesian co-ordinates.

As mentioned before, the kinematic relations (18)–(20) remain unchanged. In addition to the constitutive relations one has to make use of Maxwell's equations also which in the case of electrostatics reduce to

$$\operatorname{rot}\mathbf{E} = \mathbf{0} \tag{30}$$

and

$$\operatorname{div}\mathbf{D} = 0. \tag{31}$$

In Ref. [1], the validity of the assumption of these simplified relations examined in detail. The irrotational nature of the electric field $\mathbf{E}$ is assured if one expresses $\mathbf{E}$ through an electric potential function Φ. In the particular case of separability of the potential function this leads to

$$\mathbf{E} = -\operatorname{grad}\Phi(x,\varphi,r) = -\operatorname{grad}[\Phi_x(x)\Phi_\varphi(\varphi)\Phi_r(r)]. \tag{32}$$

Separability will be assured for the shells considered in this paper, as discussed later. In cylindrical co-ordinates Eq. (31) is written as

$$\operatorname{div}\mathbf{D} = \frac{\partial D_x}{\partial x} + \frac{1}{r}\frac{\partial D_\varphi}{\partial \varphi} + \frac{1}{r}\frac{\partial (rD_r)}{\partial r}. \tag{33}$$

Since, the polarization of the piezoelectric shell is assumed to be in the radial direction, only shear deformations could lead to electrical displacements orthogonal to the radial direction. Since they

are not considered in the kinematic relations, therefore, Eq. (33) simplifies to

$$\operatorname{div}\mathbf{D} = \frac{1}{r}\frac{\partial(rD_r)}{\partial r}. \tag{34}$$

In addition, also the components of the electric field in the circumferential direction can be disregarded and the potential is constant in the axial direction on the electrodes, so that the electrical field has no axial component. Thus, the radial component of $\mathbf{D}$ can be obtained with Eq. (26), which simplifies to

$$D_r = e_{31}S_1 + e_{31}S_2 + e_{33}S_3 + \epsilon_{33}^S E_3. \tag{35}$$

The expression for $\operatorname{div}\mathbf{D}$ becomes

$$\begin{aligned}\operatorname{div}\mathbf{D} &= \frac{1}{r}\frac{\partial}{\partial r}(r(e_{31}S_1 + e_{31}S_2 + e_{33}S_3 + \epsilon_{33}^S E_3))\\ &= \frac{1}{r}\frac{\partial}{\partial r}(r(e_{31}\varepsilon_x + e_{31}\varepsilon_\varphi + e_{33}\varepsilon_r - \epsilon_{33}^S \Phi_{,r})).\end{aligned} \tag{36}$$

Taking into account the relation

$$\varepsilon_r = -\frac{c_{13}}{c_{33}}(\varepsilon_x + \varepsilon_\varphi) - \left(2\frac{c_{13}}{c_{33}}d_{31} + d_{33}\right)\Phi_{,r}, \tag{37}$$

which holds for planar stresses, leads to

$$\operatorname{div}\mathbf{D} = \frac{1}{r}\frac{\partial}{\partial r}(r((e_{31} - e_{33}\kappa_c)(\varepsilon_x + \varepsilon_\varphi) - (2\kappa_c e_{33}d_{31} + e_{33}d_{33} + \epsilon_{33}^S)\Phi_{,r})) \tag{38}$$

with $\kappa_c = c_{13}/c_{33}$. Using the kinematic relations (19)–(21) yields

$$\begin{aligned}\operatorname{div}\mathbf{D} = &\frac{1}{ar}\frac{\partial}{\partial r}(r(e_{31} - e_{33}\kappa_c)(u_{,\vartheta} + w_{,\vartheta\vartheta} + v_{,\varphi} + w_{,\varphi\varphi}))\\ &- \frac{1}{a^2 r}\frac{\partial}{\partial r}(r^2(e_{31} - e_{33}\kappa_c)w_{,\vartheta\vartheta}) + \frac{1}{r}\frac{\partial}{\partial r}((e_{31} - e_{33}\kappa_c)(w_{,\varphi\varphi} + w))\\ &- \frac{1}{r}\frac{\partial}{\partial r}(r(2\kappa_c e_{33}d_{31} + e_{33}d_{33} + \epsilon_{33}^S)\Phi_{,r}).\end{aligned} \tag{39}$$

Condition (31) results in the differential equation

$$\begin{aligned}&\frac{1}{ar}(e_{31} - e_{33}\kappa_c)(u_{,\vartheta} + w_{,\vartheta\vartheta} + v_{,\varphi} + w_{,\varphi\varphi}) - \frac{2}{a^2}(e_{13} - e_{33}\kappa_c)w_{,\vartheta\vartheta} + \frac{0}{r}\\ &\quad = \frac{2\kappa_c e_{33}d_{13} + e_{33}d_{33} + \epsilon_{33}^S}{r}(\Phi_{,r} + r\Phi_{,rr})\end{aligned} \tag{40}$$

for the electric potential Φ. This is an inhomogeneous differential equation of the Euler type which can be written in the form

$$(\Phi_{,r} + r\Phi, rr) = \kappa_{\Phi 0} + \kappa_{\Phi 1}r, \tag{41}$$

where the abbreviations

$$\kappa_{\Phi 0} = \frac{(e_{31} - e_{33}\kappa_c)(u_{,\vartheta} + w_{,\vartheta\vartheta} + v_{,\varphi} + w_{,\varphi\varphi})}{a(2\kappa_c e_{33}d_{31} + e_{33}d_{33} + \epsilon_{33}^S)} \tag{42}$$

and

$$\kappa_{\Phi 1} = -\frac{2(e_{31} - e_{33}\kappa_c)w_{,\vartheta\vartheta}}{a^2(2\kappa_c e_{33}d_{31} + e_{33}d_{33} + \epsilon_{33}^S)} \tag{43}$$

were used. The terms $\kappa_{\Phi 0}$ and $\kappa_{\Phi 1}$ depend only on the variables x and φ through the displacements u, v and w. The general solution of the homogeneous differential equation is

$$\Phi_{rh} = C_{R1} \ln r + C_{R2} \tag{44}$$

and a particular solution of the inhomogeneous equation is given by

$$\Phi_p = \frac{\kappa_{\Phi 1}}{4} r^2 + \kappa_{\Phi 0} r, \tag{45}$$

so that the general solution of Eq. (41) is

$$\begin{aligned} \Phi(x, \varphi, r) &= \Phi_x \Phi_\varphi \Phi_{rh} + \Phi_p \\ &= \Phi_x \Phi_\varphi (C_{R1} \ln\ r + C_{R2}) + \frac{\kappa_{\Phi 1}}{4} r^2 + \kappa_{\Phi 0} r. \end{aligned} \tag{46}$$

The integration constants are determined from the boundary conditions $\Phi_r(a - \frac{s}{2}) = 0$ and $\Phi_r(a + \frac{s}{2}) = \Phi_{boundary}(x, \varphi)$ for the electric potential, so that the electric potential in the shell as function of r is given by

$$\begin{aligned} \Phi(x, \varphi, r) = &\frac{2r - 2a + s}{8}\left(4\kappa_{\Phi 0} + \kappa_{\Phi 1}\left(a + r - \frac{s}{2}\right)\right) \\ &+ \left(\Phi_{boundary} - \kappa_{\Phi 0} s - \kappa_{\Phi 1} a \frac{s}{2}\right) \frac{\ln(2a - s)/2r}{\ln(2a - s)/(2a + s)}. \end{aligned} \tag{47}$$

Here again, the logarithmic terms are replaced by the first two members of the Taylor series (see Section 2.2).

Substituting Eq. (47) into Eq. (32), using, Eqs. (27)–(29) and Eqs. (1)–(6) finally leads to the equations of motion of the piezoceramic shell in the operator form

$$\mathscr{M}[\ddot{\mathbf{w}}] + \mathscr{K}[\mathbf{w}] = \mathscr{F}(\Phi_{boundary}) \cos \Omega t, \tag{48}$$

with

$$[\mathbf{w}] = [u, v, w]^{\mathrm{T}}, \tag{49}$$

$$\mathscr{M} = (m_{ik}), \quad m_{ik} = -\mu a \delta_{ik} \tag{50}$$

and

$$\mathscr{K} = \begin{pmatrix} k_{11} & k_{12} & k_{13} \\ k_{21} & k_{22} & k_{23} \\ k_{31} & k_{32} & k_{33} \end{pmatrix}. \tag{51}$$

The elements of the operator matrix $\mathscr{K}$ and the vector $\mathscr{F}(\Phi_{boundary})$ are presented in the appendix.

3. Solution of the differential equations

The solution of Eq. (48) is 2π-periodic in the angle co-ordinate φ. Since the model is linear, superposition is permitted and any time and/or space periodic excitation can be developed in a Fourier series. The system response of the time periodic excitation is obtained by superimposing each component of the system response of the Fourier series. Solutions can be found in the form

$$u = U\mathrm{e}^{\lambda\vartheta}\cos(m\varphi)\sin(\Omega t), \tag{52}$$

$$v = V\mathrm{e}^{\lambda\vartheta}\sin(m\varphi)\sin(\Omega t), \tag{53}$$

$$w = W\mathrm{e}^{\lambda\vartheta}\cos(m\varphi)\sin(\Omega t). \tag{54}$$

For the complete solution, an orthogonal mode has also to be taken into account, which is phase shifted by $\varphi = \frac{\pi}{2}$, i.e.,

$$\bar{u} = \bar{U}\mathrm{e}^{\lambda\vartheta}\sin(m\varphi)\sin(\Omega t), \tag{55}$$

$$\bar{v} = \bar{V}\mathrm{e}^{\lambda\vartheta}\cos(m\varphi)\sin(\Omega t), \tag{56}$$

$$\bar{w} = \bar{W}\mathrm{e}^{\lambda\vartheta}\sin(m\varphi)\sin(\Omega t). \tag{57}$$

Since, Eqs. (55)–(57) do not add new information with respect to the eigenfrequencies and the eigenmodes, they are not considered any longer. The general solution for the harmonically forced case can be expressed by

$$u = \sum_i \sum_m U_{im}\mathrm{e}^{\lambda_{im}\vartheta}\cos(m\varphi)\sin(\Omega t), \tag{58}$$

$$v = \sum_i \sum_m V_{im}\mathrm{e}^{\lambda_{im}\vartheta}\sin(m\varphi)\sin(\Omega t), \tag{59}$$

$$w = \sum_i \sum_m W_{im}\mathrm{e}^{\lambda_{im}\vartheta}\cos(m\varphi)\sin(\Omega t). \tag{60}$$

In order to solve for U, V, W, Eqs. (52)–(54) are substituted into Eq. (48). Comparing the coefficients of $\cos(m\varphi)\sin(\Omega t)$ and $\sin(m\varphi)\sin(\Omega t)$ from both sides, one finally gets a set of algebraic equations which can be written in the matrix form

$$\mathbf{A}(\lambda, m, \Omega)\begin{pmatrix} U \\ V \\ W \end{pmatrix} = \mathbf{f}(\Phi_{boundary}). \tag{61}$$

The general solution of the above algebraic equations contains the solution of the homogeneous problem (denoted by $\mathbf{U}_h$) and the particular solution (denoted by $\mathbf{U}_p$). The homogeneous set of equations of free vibration with short-circuited electrodes takes the form (for convenience the

subscript h is temporarily omitted)

$$\mathbf{A}(\lambda, m, \omega)\begin{pmatrix} U \\ V \\ W \end{pmatrix} = \mathbf{0}. \tag{62}$$

The characteristic equation of the eigenvalue problem is obtained as

$$\sum_{i}^{8}\sum_{j}^{8}\sum_{k}^{6} a_{ijk}\lambda^i m^j \omega^k = 0. \tag{63}$$

Polynomial (63) represents the dispersion relation and is of the order of 8 in λ^i and m^j and of 6 in ω^k, more precisely, it is of the order 4 in λ^{2i} and m^{2j} and of 3 in ω^{2k}. In general m which can take only integer values, gives the number of wavelengths of the travelling waves around the circumference. For each pair of ω and m, eight sets of solutions for λ_i and their corresponding vectors $(U_i, V_i, W_i)^{\mathrm{T}}$ are obtained. The eigenfunction can be written by superimposing the above solutions where the unknown coefficients are determined up to a constant factor by satisfying the boundary conditions. For a free–free vibrating cylindrical shell, the boundary conditions at each free end are obtained from vanishing normal forces $(N_x, N_{x\varphi})$ and equivalent shear forces $(V_x, V_{x\varphi})$:

$$V_x = Q_x - \frac{1}{a} M_{x\varphi,\varphi}, \tag{64}$$

$$V_{x\varphi} = N_{x\varphi} + \frac{1}{a} M_{x\varphi}. \tag{65}$$

The boundary conditions then yield the algebraic matrix equation

$$\mathbf{M}(\lambda_i(\omega), \mathbf{U}_i(\omega))\mathbf{1} = \mathbf{0}. \tag{66}$$

The determinant of $\mathbf{M}$, which is a function of ω must vanish for the eigenfrequencies. The corresponding eigenvector $\mathbf{1}$ contains the coefficients of $\mathbf{U_i} = (U_i, V_i, W_i)^{\mathrm{T}}$. Therewith, the solution of the homogeneous problem is obtained. In the following, the particular solution of the inhomogeneous problem will be derived.

For the particular solution the relation

$$\mathbf{U}_p = \mathbf{A}^{-1}(\lambda, m, \Omega)\mathbf{f}(\Phi_{boundary}) \tag{67}$$

holds. Analogous to the free vibrations of the shell, the solutions of Eq. (61) are found applying the frequency Ω of the excitation $\mathbf{f}(\Phi)$. The boundary conditions are formulated as

$$\mathbf{M}(\lambda_i(\Omega), \mathbf{U}_i(\Omega))\mathbf{1} = -\mathbf{M}_e - \mathbf{M}(\Lambda, \mathbf{U}_p), \tag{68}$$

where in the right-hand side, the vector $\mathbf{M}_e$ comes directly from the electrical excitation and the second vector $\mathbf{M}(\Lambda, \mathbf{U}_p)$ contains the particular solution. Λ is obtained by the relation

$$\Phi_{boundary} = \hat{\Phi} \mathrm{e}^{\Lambda\vartheta} \cos m\varphi \sin \Omega t. \tag{69}$$

Since the electrical potential is independent of x, Λ turns out to be zero. The coefficients of the eight sets of solutions of vector $\mathbf{U}$ are calculated with

$$\mathbf{1} = -\mathbf{M}^{-1}(\lambda_i(\Omega), \mathbf{U}_i(\Omega))(\mathbf{M}_e + \mathbf{M}(\Lambda, \mathbf{U}_p)), \tag{70}$$

so that finally, the complete solution of the inhomogeneous problem is

$$\mathbf{U} = \mathbf{U}_p + \mathbf{1}\,\mathbf{U}_h. \tag{71}$$

4. Electrical admittance

In a piezoelectric shell it is usually easier to measure the electrical impedance or admittance via an impedance analyzer than the eigenmodes and eigenfrequencies via experimental modal analyzers. Therefore, the admittance will be computed to verify the model.

To compute the electrical admittance Y of a system, the surface charge of the electrodes and the potential are needed. Other than in the piezoelectric material where $\operatorname{div}\mathbf{D}$ vanishes, in the electrode $\operatorname{div}\mathbf{D} = \varrho_Q$, where ϱ_Q is an expression for the density of free charges. With

$$I = \dot{Q}, \quad Q = \int_{electrode}\int\int \varrho_Q \,\mathrm{d}V = \int_{electrode}\int\int \operatorname{div}\mathbf{D}\,\mathrm{d}V \tag{72}$$

and

$$\hat{U} = \hat{\Phi}|_{z=-s/2}^{z=s/2}, \tag{73}$$

the electrical admittance can be written as

$$Y = \frac{\hat{I}}{\hat{U}}$$

with $\hat{I}$, $\hat{U}$ as the complex amplitudes of the harmonic current and voltage, respectively. This leads to

$$Y = \frac{\int_{electrode}\int\int \operatorname{div}\hat{\mathbf{D}}\,\mathrm{d}V}{\hat{\Phi}_{boundary}}. \tag{74}$$

Using Gauss' law, the charge contained inside a control volume (see Fig. 3) is related to the electrical displacement bounded by a surface and is expressed by

$$\int_{electrode}\int\int \operatorname{div}\hat{\mathbf{D}}\,\mathrm{d}V = \int_{electrode}\int \hat{\mathbf{D}}\cdot\mathbf{n}\,\mathrm{d}A, \tag{75}$$

where $\mathbf{n}$ is the normal vector of the surface. In the limiting case, one surface in the piezo material and another parallel surface in the electrode material are to be considered, only. Due to a very

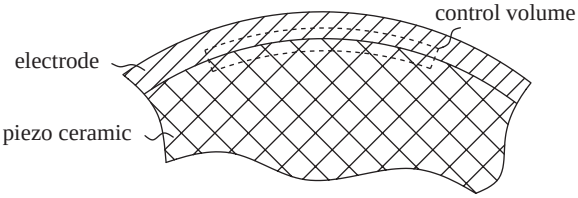

Fig. 3. Control volume to acquire the surface charge.

high conductivity of the electrode material, the electric field within the electrode is negligible. Thus, the electric displacement in the electrode vanishes and plays no role in the surface integral Eq. (54). Hence, the surface integral is to be evaluated only over the surface within the piezo material.

The normal vector $\mathbf{n}$ has the radial component only. Thus, the term of the integral in Eq. (54) simplifies to

$$\hat{\dot{\mathbf{D}}} \cdot \mathbf{n} = \begin{cases} \hat{\dot{D}}_r & \text{for } r = a - s/2, \\ -\hat{\dot{D}}_r & \text{for } r = a + s/2. \end{cases} \tag{76}$$

For harmonically excited systems

$$\hat{\dot{\mathbf{D}}} - \imath\Omega\hat{\mathbf{D}} \tag{77}$$

holds and therefore, the electrical admittance yields

$$Y = \frac{\imath\Omega \int\int_{electrode} \hat{D}_r \, \mathrm{d}A}{\hat{\Phi}_{boundary}}. \tag{78}$$

5. Results

Numerical results obtained from the described piezo-shell model are compared to those from experiments obtained in our lab. Displacements, admittances and eigenmodes are presented and discussed.

5.1. Admittance

For the measurement of the admittances one set of electrodes of the piezoceramic ring is excited by applying a harmonic voltage signal. Both other sets of electrodes are short-circuited with the inner electrode. The advantage of having the electrodes short-circuited is that the boundary conditions are potential boundary conditions which can be locally formulated. With open electrodes, the boundary conditions would be charge boundary conditions which are only amenable to an integral description.

Fig. 4 presents admittances calculated from the model and obtained from the experiment. The electrical admittances were obtained using the Impedance/Gain-Phase Analyzer HP 4194A together with the Measurement Unit HP 4194A. The frequencies 88 and 159 kHz, which were calculated from the model, correspond to the first and second eigenfrequency of the piezoring and are verified through the experimental results. Their deflection to the experimentally obtained resonance frequencies is $\approx 4\%$. This is perfectly acceptable since the material constants are specified by the manufacturer with an error margin of 5%. No attempt was made to match computational results to experimental data by adjusting parameters. The measured admittances at the points of resonance could not be verified by the model since quality factors for piezoceramics given by manufacturers were very imprecise.

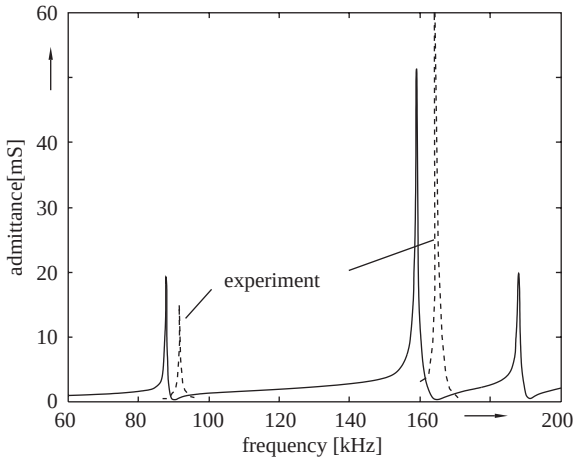

Fig. 4. Admittances—model and experiment.

5.2. Axial displacements

In order to assure a good approximation to the free–free boundary conditions at both ends of the piezoelectric shell in the experiment, a clamp with soft rubber was built which holds the ring by small axisymmetric outward radial forces on the inner surface. The clamp construction was mounted on a rotating table to make all points accessible for measuring the displacements. The velocity points on the surface of the shell were measured using the Laser Vibrometer, POLYTEC OFV 2802 and OFV 508.

The piezoshell was excited by one set of electrodes while the two remaining sets were short-circuited for reasons explained in Section 5.1. Measurements of the surface velocities in axial and radial direction were taken at one location of the shell. Finishing the measurements at one location, the piezoceramic was turned by a defined angle of $5-10^{\circ}$ and recording of the measurements of displacements was continued. One set of measured data is then a characteristic diagram of the transfer function of excitation voltage to surface velocities. In Fig. 5 axial displacements over the circumference of the shell from both experiment and model are shown for the first eigenfrequency of $f \approx 89$ kHz.

For the axial displacement at the first eigenfrequency, the computation stands in good agreement to what was measured. The calculation is based on the material constants and geometric parameters given in the appendix.

5.3. Eigenmodes of the piezo ceramic shell

In this section, the computed vibration modes are visualized. In Figs. 6 and 7, the vibration modes of the first two eigenfrequencies are shown. The displacements are scaled to aid visualization. The axial displacements at the first eigenfrequency of approximately 89 kHz (Fig. 6) are relatively small compared to those of the second eigenfrequency (Fig. 7). In contrast, the radial part of displacements at the first eigenfrequency are higher than those at the second

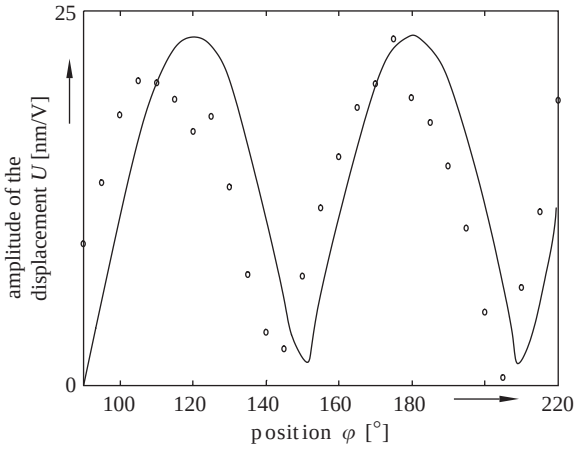

Fig. 5. Axial displacement at $f \approx 89$ kHz.

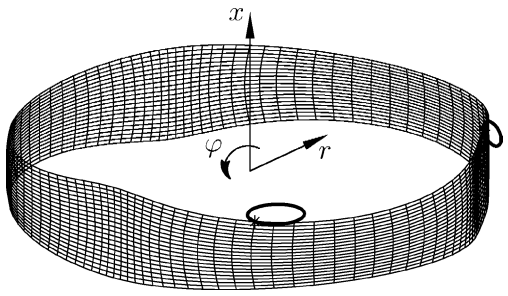

Fig. 6. First eigenmode at $f \approx 89$ kHz.

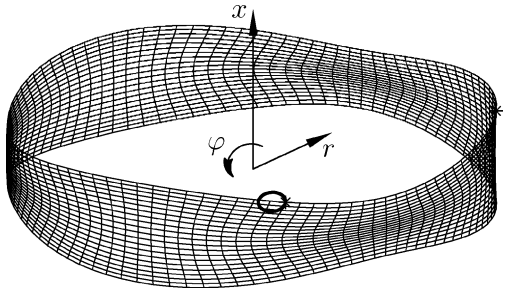

Fig. 7. Second eigenmode at $f \approx 159$ kHz.

frequency. This may be important for the piezoceramic motor using the shell as a stator. The radial motion is perpendicular to the generalized elliptical motion and hinders the rotatory motion of the rotor. So, for a motor application the second eigenmode is recommended.

6. Conclusions

In this paper Flügge's equations for cylindrical shells were generalized to the case of piezoelectric shells polarized in the radial direction. Such shells are used e.g., as stators in some piezoelectric ultrasonic travelling wave motors and it is therefore important to study their free and forced vibrations. The constitutive relations used in the theory of elastic shells were replaced by those of a linear piezoelectric material. Therefore, additional field variables were introduced. Together with Flügge's thin shell assumptions and with the piezoceramic constitutive equations this resulted in the new equations of motion of a thin piezoceramic shell. Our shell equations differ from those known from the literature, in that, we do not assume the electric field as constant over the thickness.

For the case of a set of electrodes in the form of axial strips placed at equal angular differences around the circumference and excited by a voltage, the equations of motion were solved using Fourier techniques. Electrical admittances and the resonance frequencies were computed as well.

Eigenmodes and eigenfrequencies were obtained and compared to experimental values. The experiments were carried out in the department's laboratory using laser vibrometers and impedance analyzers.

The proposed model of the shell stands in good agreement with the experiment and can be used in modelling a larger integrated system, like ultrasonic motor, of which it is an important member.

This is an alternative to the use of 3-D FEM calculations for shells and gives a useful engineering tool for a number of problems involving piezoelectric actuators. It offers also a basis for the formulation of a new type of finite element with non-constant electric field. Such new elements may be useful for 2-D FE calculations of piezoelectric, monolythic structure and piezoelectric shells.

Acknowledgements

The authors would like to thank the VolkswagenStiftung for support given to this project.

Appendix

Material matrices of the piezoceramic type PIC141

$$\mathbf{c}^E = \begin{pmatrix} c_{11} & c_{12} & c_{13} & 0 & 0 & 0 \\ c_{12} & c_{11} & c_{13} & 0 & 0 & 0 \\ c_{13} & c_{13} & c_{33} & 0 & 0 & 0 \\ 0 & 0 & 0 & c_{44} & 0 & 0 \\ 0 & 0 & 0 & 0 & c_{44} & 0 \\ 0 & 0 & 0 & 0 & 0 & c_{66} \end{pmatrix} \quad \text{with } c_{66} = \tfrac{1}{2}(c_{11} - c_{12}),$$

$$\mathbf{d} = \begin{pmatrix} 0 & 0 & 0 & 0 & d_{15} & 0 \\ 0 & 0 & 0 & d_{15} & 0 & 0 \\ d_{31} & d_{31} & d_{33} & 0 & 0 & 0 \end{pmatrix},$$

$$\mathbf{e} = \mathbf{d}\mathbf{c}^E,$$

$$\boldsymbol{\epsilon}^S = \begin{pmatrix} \epsilon_{11} & 0 & 0 \\ 0 & \epsilon_{11} & 0 \\ 0 & 0 & \epsilon_{33} \end{pmatrix}.$$

Material constants of the piezoceramic type PIC141 and geometric parameters of the shell:

ε_{11}	1.328×10^{-8}	$A^2\ s^4\ kg^{-1}\ m^{-3}$
ε_{33}	1.151×10^{-8}	$A^2\ s^4\ kg^{-1}\ m^{-3}$
c_{11}	1.077×10^{11}	$kg\ m^{-1}\ s^{-2}$
c_{33}	1.047×10^{11}	$kg\ m^{-1}\ s^{-2}$
c_{12}	4.664×10^{10}	$kg\ m^{-1}\ s^{-2}$
c_{13}	4.630×10^{10}	$kg\ m^{-1}\ s^{-2}$
d_{31}	-1.15×10^{-10}	$A\ s^3\ kg^{-1}\ m^{-1}$
d_{33}	3.30×10^{-10}	$A\ s^3\ kg^{-1}\ m^{-1}$
d_{15}	4.75×10^{-10}	$A\ s^3\ kg^{-1}\ m^{-1}$
e_{31}	-2.47	$A\ s\ m^{-2}$
e_{33}	23.90	$A\ s\ m^{-2}$

Axial height	h	10 mm
Mid-radius	a	18 mm
Shell thickness	s	2 mm

Elements of operator matrix $\mathscr{K}$

$$k_{11} = \kappa_1 \frac{s}{2a}\left(-\frac{(12a^2+s^2)}{12a^2}\frac{\partial^2}{\partial\varphi^2} - 2\frac{\partial^2}{\partial\vartheta^2}\right) + \kappa_2 \frac{s}{2a}\frac{(12a^2+s^2)}{12a^2}\frac{\partial^2}{\partial\varphi^2} - \kappa_p \frac{s}{a}\frac{s^2}{(12a^2+s^2)}\frac{\partial^2}{\partial\vartheta^2},$$

$$k_{21} = -\kappa_2 \frac{s}{2a}\frac{\partial^2}{\partial\varphi\partial\vartheta} - \kappa_1 \frac{s}{2a}\frac{\partial^2}{\partial\varphi\partial\vartheta} - \kappa_p \frac{s^3}{(12a^3+s^2a)}\frac{\partial^2}{\partial\varphi\partial\vartheta},$$

$$k_{31} = \kappa_1 \frac{s^3}{24a^3}\left(\frac{\partial^3}{\partial\vartheta\partial\varphi^2} - 2\frac{\partial^3}{\partial\vartheta^3}\right) + \kappa_2 \frac{s}{2a}\left(2\frac{\partial}{\partial\vartheta} - \frac{s^2}{12a^2}\frac{\partial^3}{\partial\vartheta\partial\varphi^2}\right)$$
$$- \kappa_p \frac{s^3}{a}\left(\frac{1}{(12a^2+s^2)}\frac{\partial^3}{\partial\vartheta\partial\varphi^2} + \frac{1}{12a^2}\frac{\partial^3}{\partial\vartheta^3}\right),$$

$$k_{12} = \kappa_1 \frac{s}{2a}\frac{\partial^2}{\partial\vartheta\partial\varphi} - \kappa_2 \frac{s}{2a}\frac{\partial^2}{\partial\vartheta\partial\varphi} - \kappa_p \frac{s^3}{(12a^3 + s^2a)}\frac{\partial^2}{\partial\vartheta\partial\varphi},$$

$$k_{22} = -\kappa_1\frac{s}{2a}\left(2\frac{\partial^2}{\partial\varphi^2} + \frac{(4a^2+s^2)}{4a^2}\frac{\partial}{\partial\vartheta^2}\right) + \kappa_2\frac{(4sa^2+s^2)}{8a^3}\frac{\partial^2}{\partial\vartheta^2} - \kappa_p\frac{s^3}{(12a^3+s^2a)}\frac{\partial^2}{\partial\varphi^2},$$

$$k_{32} = -\kappa_1\frac{s^3}{sa^3}\frac{\partial^3}{\partial\vartheta^2\partial\varphi} + \kappa_1\frac{s}{a}\frac{\partial}{\partial\varphi} + \kappa_2\frac{s^3}{24a^3}\frac{\partial^3}{\partial\vartheta^2\partial\varphi} - \kappa_p\frac{s^3}{a}\left(\frac{1}{(12a^2+s^2)}\frac{\partial^3}{\partial\varphi^3} + \frac{1}{12a^2}\frac{\partial^3}{\partial\vartheta^3}\right),$$

$$k_{13} = \kappa_1\frac{s^3}{24a^3}\left(-\frac{\partial^3}{\partial\vartheta\partial\varphi^2}\right) + \kappa_2\left(-\frac{s}{a}\frac{\partial}{\partial\vartheta} + \frac{s^3}{24a^3}\frac{\partial^3}{\partial\vartheta\partial\varphi^2}\right) + \kappa_p\frac{s^3}{a}\left(-\frac{1}{(12a^2+s^2)}\frac{\partial^3}{\partial\vartheta^2\partial\varphi} + \frac{1}{12a^2}\frac{\partial^3}{\partial\vartheta^3}\right),$$

$$k_{23} = \kappa_1\frac{s}{2a}\left(-2\frac{\partial}{\partial\varphi} + \frac{s^2}{4a^2}\frac{\partial^3}{\partial\vartheta^2\partial\varphi}\right) - \kappa_2\frac{s^3}{24a^3}\frac{\partial^3}{\partial\vartheta^2\partial\varphi} + \kappa_p\frac{s^3}{a}\left(-\frac{1}{(12a^3+s^2)}\frac{\partial^3}{\partial\varphi^3} + \frac{1}{12a^2}\frac{\partial^3}{\partial\vartheta^2\partial\varphi}\right),$$

$$k_{33} = \kappa_1\frac{s^2}{24a^3}\left(4\frac{\partial^2}{\partial\varphi^2} + 2\frac{\partial^4}{\partial\varphi^4} + 4\frac{\partial^4}{\partial\vartheta^2\partial\varphi^2} + 2\frac{\partial^4}{\partial\vartheta^4} + 2\right) + \kappa_2\frac{s}{a} + \kappa_p\frac{s^3}{a}\left(-\frac{1}{(12a^2+s^2)}\frac{\partial^4}{\partial\varphi^4} + \frac{1}{12a^2}\frac{\partial^4}{\partial\vartheta^4}\right).$$

Vector $\mathscr{F}$:

$$\mathscr{F} = \begin{pmatrix} \dfrac{12a^2}{(12a^2+s^2)}\kappa_d\dfrac{\partial}{\partial\vartheta} \\ \dfrac{12a^2}{(12a^2+s^2)}\kappa_d\dfrac{\partial}{\partial\varphi} \\ -\left(1 + \dfrac{s^2}{(12a^2+s^2)}\dfrac{\partial^2}{\partial\varphi^2}\right) \end{pmatrix}\Phi_{boundary}.$$

Constants:

according to Flügge :	defined in this paper :
$\kappa_1 = -\dfrac{D}{s} = \dfrac{E}{(\nu^2-1)},$	$\kappa_1 = \dfrac{c_{13}^2}{c_{33}} - c_{11},$
$\kappa_2 = -\nu\dfrac{D}{s} = \dfrac{\nu E}{(\nu^2-1)},$	$\kappa_2 = \dfrac{c_{13}^2}{c_{33}} - c_{12},$
$\kappa_d = 0,$	$\kappa_d = d_{13}(\kappa_1+\kappa_2),$
$\kappa_p = 0.$	$\kappa_p = -\dfrac{\kappa_d^2}{[(2c_{13}d_{13}+c_{33}d_{33})^2 + c_{33}\epsilon_{33}^S]}.$

For non-piezoelectric material substituting $\mathbf{d} = \mathbf{0}$ and modifying the stiffness matrix by taking care of the simplification for isotropic material, one gets back Flügge equations of motion.

References

[1] M. Berg, Ein Wanderwellenmotor mit zylindrischem Stator: Mathematische Modellierung und experimentelle Untersuchung, PhD Thesis, Darmstadt University of Technology, 2002.
[2] M. Berg, P. Hagedorn, A note on minimization of electrical losses in controllers of piezoelectric motors, *Proceedings of Actuator 2000*, 2000.
[3] E.F. Crawley, E.H. Anderson, Detailed models of piezoceramic actuation of beams, *American Institute of Aeronautics and Astronautics Journal* 89 (1989) 1388-CP.
[4] E.F. Crawley, J. de Luis, Use of piezoelectric actuators as elements of intelligent structures, *American Institute of Aeronautics and Astronautics Journal* 25 (10) (1987) 1373–1385.
[5] E.F. Crawley, K.B Lazarus, Induced strain actuation of isotropic and anisotropic plates, *American Institute of Aeronautics and Astronautics Journal* 29 (6) (1991) 944–951.
[6] E.K. Dimitriadis, C.R. Fuller, C.A. Rogers, Piezoelectric actuators for distributed vibration excitation of thin plates, *Transaction of American Society of Mechanical Engineering, Journal of Vibration and Acoustics* 113 (1991) 100–107.
[7] C.-K. Lee, Theory of laminated piezoelectric plates for the design of distributed sensors/actuators. Part i: Governing equations and reciprocal relationships, *Journal of the Acoustical Society of America* 87 (3) (1990) 1144–1158.
[8] W. Flügge, *Statik und Dynamik der Schalen*, Springer, Berlin, 1962.
[9] W. Flügge, *Stresses in Shells*, 2nd Edition, Springer, Berlin, April 1973.
[10] T. Ikeda, *Fundamentals of Piezoelectricity*, Oxford University Press, Oxford, 1990.
[11] K.-D. Wolf, Electromechanical Energy Conversation in Asymmetric Piezoelectric Bending Actuators, PhD Thesis, Darmstadt University of Technology, 2000.